

Motion and Stability of a Dual-Spin Satellite with Nutation Damping

P. M. BAINUM,* P. G. FUECHSEL,† AND D. L. MACKISON‡

The Johns Hopkins University, Applied Physics Laboratory, Silver Spring, Md.

The damping and stability characteristics of a dual spin satellite system are analyzed. The system consists of: a slowly rotating main part; a high speed rotor whose spin axis is parallel to the nominal main body spin axis; and one or two pendulous type nutation dampers, pivoted about a torsion wire support and constrained to move in a plane that is perpendicular to the nominal spin axis. After development and linearization of the equations of motion, the necessary and sufficient Routh-Hurwitz stability criteria are obtained. The damping system design is optimized by repeated examination of the roots of the system characteristic equation. Numerical studies using the nonlinear equations are conducted to evaluate the spin axis pointing error attributed to the dynamic mass unbalance of the main body in a torque-free environment. It is found that this results in a noticeable degradation in nutation damping performance.

Nomenclature

$\bar{A}, \bar{B}, \bar{C}$	= composite moments of inertia about the x, y, z axes, respectively
\bar{b}_i	= unit vectors along the x, y, z axes, respectively, ($i = 1, 2, 3$)
C_i	= coefficients occurring in linearized equations
I_{b_i}	= moment of inertia of main body about the \bar{b}_i axis
I_{R_i}	= moment of inertia of rotor about its \bar{b}_i axis
I_{d_i}	= moment of inertia of the pendulous damper(s) about the \bar{b}_i axis
K	= the restoring spring constant of the torsion wire support
\bar{K}	= $K/mr_1^2\Omega^2$, dimensionless form of K
k	= the damping (rate) constant
\bar{k}	= $k/mr_1^2\Omega$, dimensionless form of k
l	= height of damper plane above x, z plane
L_i	= the applied external torques about the \bar{b}_i axis
M	= the mass of the main satellite and the rotor
\bar{M}	= the total system mass
m	= the pendulum end mass
Q_i	= the generalized forces occurring in the ϕ_i equations
r_0	= the distance from the nominal spin (y) axis to the pendulum hinge point
r_1	= the length of the pendulum
s	= spin rate of rotor relative to main body
T	= kinetic energy
t	= time
V	= potential energy associated with restoring torque effects
u	= nondimensionalized form of ω_3
v	= nondimensionalized form of ω_1
x, y, z	= principal axes of main satellite
α	= variation of angular velocity, ω_3 , from nominal value, Ω
Ω	= nominal main body spin rate
ϕ_i	= damper displacement angles, ($i = 1, 2$)
ω_0	= orbital angular velocity

ω_i	= angular velocities about the x, y, z axes, respectively ($i = 1, 2, 3$)
τ	= Ω dimensionless time

Superscripts

()'	indicates differentiation with respect to τ
()	indicates differentiation with respect to t

Subscript

b_i, i	refers to particular body axes, ($i = 1, 2, 3$)
----------	---

I. Introduction

HASELTINE¹ and others at the Naval Ordnance Test Station have treated the problem of nutation damping rates for a single part spinning satellite having pendulous type nutation dampers that are free to move in a plane that is normal to the desired spin axis of the satellite. Initial perturbations will cause a "wobbling" or nutation of the spin axis which would persist indefinitely in the absence of damping. By proper selection of the damping system parameters it is possible to achieve very rapid damping of the half-cone angle associated with the initial nutation.

A dual-spin spacecraft may be considered to consist of two bodies constrained so that the relative motion is restricted to a rotation about a common axis fixed in both bodies. A freely spinning system (consisting of two sections which rotate relative to each other) may be stable in spin about the major axis of inertia, if the larger body is constrained to rotate very slowly in inertial space while the smaller connected body (i.e., flywheel or rotor) can rotate very rapidly relative to the larger part. Furthermore, depending on the spin rate, the system may be stable in spin about an axis of least inertia in the presence of damping. The stability theory and design of dual-spin satellites with various types of passive and semiactive nutation damping systems was discussed at a recent symposium on the attitude stabilization and control of dual-spin spacecraft.²

A dual-spin Small Astronomy Satellite (SAS-A) is currently being designed and developed for the NASA Goddard Space Flight Center by the Applied Physics Laboratory with a 1970 tentative launch date scheduled. The satellite will scan the entire celestial sphere to determine the location of X-ray emitting sources relative to the fixed position of the stars. It is important that the attitude of the satellite be

Received August 18, 1969; presented as Paper 69-857 at the AIAA Guidance, Control and Flight Mechanics Conference, Princeton, N.J., August 18-20, 1969; revision received January 16, 1970. This research was supported by the NASA Goddard Space Flight Center, Contract N0w62-0604-C.

* Consulting Engineer; also, Associate Professor of Aerospace Engineering, Howard University, Washington, D.C. Member AIAA.

† Associate Engineer.

‡ Presently Staff Scientist, Ball Brothers Research Corporation, Boulder, Colo.

precisely known and maintained in order to accurately determine the location of the X-ray emitting sources. The attitude errors or drifts in a fixed time interval must be known in order to accurately determine the position of an X-ray emission which might be detected between any two star sightings (nominally to be taken at 20 sec intervals).

The present analysis is based on a dual spin configuration consisting of a slowly rotating ($\frac{1}{12}$ rpm) main body, a high-speed rotor whose spin axis is parallel to (but not necessarily collinear with) the spin axis of the main body, and one or two pendulous type nutation dampers that are constrained to move in a plane which is perpendicular to the nominal spin axes of the main satellite. This system differs from others previously considered in that the dampers are pivoted about a torsion wire support that offers a restoring torque in addition to the dissipative (damping) torque.

II. Analysis

The satellite, rotor, and damper systems are illustrated in Fig. 1. The satellite is comprised of three parts, 1) the primary part of the satellite, assumed to be essentially a right circular cylinder where the nominal spin axis is the \bar{b}_2 body axis, 2) the smaller rotor or flywheel which is assumed to be connected near the center of mass of the primary part, and whose spin axis is also along or parallel to the \bar{b}_2 body axis, and 3) the pendulous-type nutation dampers which are attached to the primary part and are constrained to move in a plane a distance l above the \bar{b}_1, \bar{b}_3 plane (determined by the body axes perpendicular to the axis of symmetry). It is assumed the dampers are hinged or pivoted about a torsion wire support which offers a restoring (spring) torque in addition to the dissipative torque.

A. Equations of Motion

The development of the equations of motion follows that of Haseltine,¹ with the following additional kinetic energy terms due to the small constant speed rotor

$$T_{\text{Rotor}} = \frac{1}{2} [I_{R2}(\omega_2 + s)^2 + I_{R1}\omega_1^2 + I_{R3}\omega_3^2] \quad (1)$$

where the rotor is assumed to be spinning about the y or \bar{b}_2 axis, with a relative angular velocity s with respect to the main spacecraft and $(\omega_1, \omega_2, \omega_3)$ are the inertial angular velocity components of the main body. The complete expression for the kinetic energy is given in a recent report.³

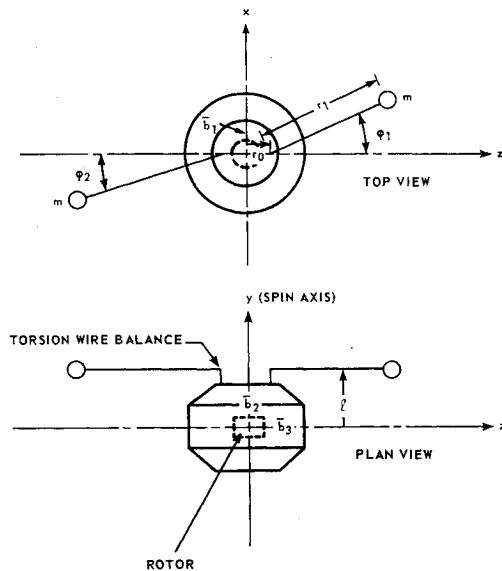


Fig. 1 Schematic of satellite, rotor, and damper.

The equations of motion for this case can thus be expressed in terms of the quasi-coordinates $(\omega_1, \omega_2, \omega_3)$ and the angles swept out (ϕ_i) by the pendulous dampers according to⁴

$$\begin{aligned} (d/dt) \partial T / \partial \omega_1 - \omega_2 \partial T / \partial \omega_2 + \omega_3 \partial T / \partial \omega_3 &= L_1 \\ (d/dt) (\partial T / \partial \omega_2) - \omega_1 \partial T / \partial \omega_3 + \omega_3 \partial T / \partial \omega_1 &= L_2 \\ (d/dt) (\partial T / \partial \omega_3) - \omega_2 \partial T / \partial \omega_1 + \omega_1 \partial T / \partial \omega_2 &= L_3 \\ (d/dt) (\partial T / \partial \dot{\phi}_i) - \partial T / \partial \phi_i + \partial \mathcal{F} / \partial \dot{\phi}_i &= Q_i; \quad i = 1 \rightarrow N \end{aligned} \quad (2)$$

where N represents the total number of pendulous dampers; the viscous drag on the pendulous end masses, which varies linearly with the angular velocity $\dot{\phi}_i$ can be derived from the Rayleigh dissipation function \mathcal{F} . In this case,

$$\mathcal{F} = \frac{1}{2} \sum_{i=1}^N (k_i \dot{\phi}_i^2) \quad (3)$$

The restoring torque on each damper provided by the torsion wire support is represented by $Q_i = -\partial V / \partial \phi_i$ where the potential energy V is proportional to the square of the angular displacement from the equilibrium position

$$V = \frac{1}{2} \sum_{i=1}^N K_i \phi_i^2 \quad (4)$$

Equation (2) may be expanded and simplified with small angle assumptions made relative to the magnitudes of the ϕ_i , and with the further assumptions that $\omega_i / \omega_2 \ll 1$, and $\dot{\phi}_i / \omega_2 \ll 1$. The following first-order equations result for the case of $N = 2$ dampers:

$$\bar{B} \dot{\omega}_2 + \omega_1 \omega_3 (\bar{A} - \bar{C}) + m r_1 (r_1 + r_0) (\ddot{\phi}_1 + \ddot{\phi}_2) = L_2 \quad (5)$$

$$\bar{A} \dot{\omega}_1 + \omega_2 \omega_3 (\bar{C} - \bar{B}) - \omega_3 I_{R2} s - 2 m \omega_2 r_1 (l M / \bar{M}) \times (\dot{\phi}_1 - \dot{\phi}_2) = L_1 \quad (6)$$

$$\bar{C} \dot{\omega}_3 + \omega_1 \omega_2 (\bar{B} - \bar{A}) + \omega_1 I_{R2} s - m r_1 (l M / \bar{M}) \times (\ddot{\phi}_1 - \ddot{\phi}_2) + m \omega_2^2 r_1 (l M / \bar{M}) (\phi_1 - \phi_2) = L_3 \quad (7)$$

$$\begin{aligned} m r_1^2 \left(1 - \frac{m}{\bar{M}} \right) \ddot{\phi}_1 + \frac{m^2 r_1^2 \ddot{\phi}_2}{\bar{M}} - m r_1 \frac{l M}{\bar{M}} \dot{\omega}_3 + \\ m r_1 (r_0 + r_1) \dot{\omega}_2 + \omega_2^2 m r_1 \left(r_0 + \frac{m r_1}{\bar{M}} \right) \phi_1 - \\ \omega_2^2 r_1^2 \frac{m^2 \phi_2}{\bar{M}} + m \omega_2 r_1 \frac{l M \omega_1}{\bar{M}} = -k \dot{\phi}_1 - K \phi_1 \end{aligned} \quad (8)$$

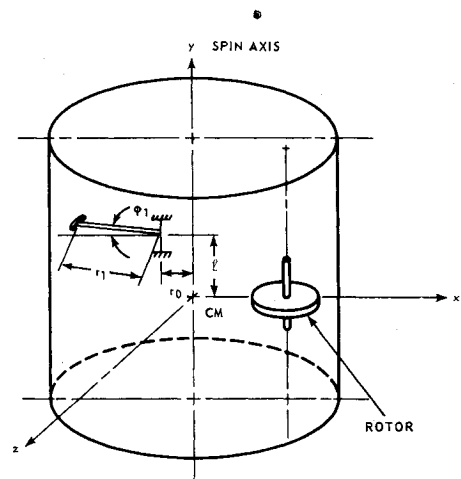


Fig. 2 Elements of SAS-A attitude control system (rotor displaced from spin axis).

$$\begin{aligned}
mr_1^2 \left(1 - \frac{m}{M}\right) \ddot{\phi}_2 + \frac{m^2 r_1^2 \dot{\phi}_1}{M} + mr_1 \frac{LM \dot{\omega}_3}{M} + \\
m_1 r_1 (r_0 + r_1) \dot{\omega}_2 + \omega_2^2 m r_1 \left(r_0 + \frac{m r_1}{M}\right) \phi_2 - \\
\omega_2^2 r_1^2 \frac{m^2 \phi_1}{M} - \frac{m \omega_2 r_1 LM \omega_1}{M} = -k \dot{\phi}_2 - K \phi_2 \quad (9)
\end{aligned}$$

where the total inertia terms have main body, rotor, and damper components

$$\begin{aligned}
\bar{A} &= I_{b1} + I_{R1} + I_{d1}, & \bar{B} &= I_{b2} + I_{R2} + I_{d2} \\
\bar{C} &= I_{b3} + I_{R3} + I_{d3}
\end{aligned}$$

for symmetrical arrangement of dampers about the nominal spin axis $\bar{C} = \bar{A}$. Equations (5-9) consider a system with two nutation dampers which, when in equilibrium, will be collinear. For small motions of either or both pendulums the system center of mass shift will be very small and need not be included as long as the pendulums are considered to be arranged in collinear pairs; the limiting case considers one pendulum free to move and the other member of the pair acting like a fixed counterweight. If a second pair of pendulums were considered there would be two additional equations of motion similar in form to Eqs. (8) and (9).

Figure 2 illustrates the actual design of the SAS-A attitude control system. It should be noted that the rotor will be displaced from the system center of mass and that the rotor spin axis will be parallel to the desired main body spin axis. In the event that a perfect static mass balance is not achieved, the axes of symmetry are not the principal axes. The nonlinear equations of motion for this system have been modified in order to represent the general misalignment of the principal axes from the geometrical axes of symmetry.³

The applied torque terms (L_1 , L_2 , L_3) include gravity-gradient, solar pressure, and other externally induced effects. For example, the gravity torque terms for the special case where the spin axis is nominally perpendicular to the orbital plane and the system center of mass describes a circular orbit can be written,

$$\begin{aligned}
L_1 &= 3\omega_0^2(\bar{C} - \bar{B})\theta \cos\phi \\
L_2 &= 3\omega_0^2(\bar{C} - \bar{A})\sin\phi \cos\phi \quad (10) \\
L_3 &= 3\omega_0^2(\bar{A} - \bar{B})\theta \sin\phi; \text{ for } \theta \ll 1
\end{aligned}$$

where θ is the "roll" angle corresponding to motions about the \bar{b}_1 axis, and ϕ represents angular displacements about the \bar{b}_2 or spin axis and is not necessarily small; the symbol ω_0 refers to the orbital angular velocity.

The nonlinear equations of motion including the effect of mass asymmetry and the generalized gravity-gradient torques have been programmed for numerical integration with the IBM 360/91 computer. A subroutine has been added which gives the orientations of the spin axis in terms of the geocentric right ascension and declination angles or, alternatively, in terms of a prescribed set of Euler angles relative to the local vertical system.

To consider the performance of the system damping for reducing initial nutations in a torque-free environment, Eqs. (5-9), with $L_1 = L_2 = L_3 = 0$, were linearized following the procedure of Haseltine.¹ The angular velocity about the nominal spin axis may be written as $\omega_2 = \Omega + \alpha$ with Ω , the nominal spin rate as a constant, and regarding α/Ω as small. Equation (5) can then be used to eliminate $\dot{\alpha}$ from the other equations. The resulting set of linearized equations with constant coefficients result

$$C_{1u}' + C_2 v + C_3(\phi_1'' - \phi_1) + C_4(\phi_2'' - \phi_2) = 0 \quad (11)$$

$$C_{5u} + C_{6v}' + C_7(\phi_1' - \phi_2') = 0 \quad (12)$$

$$C_8 u' + C_9 v + C_{10} \phi_1'' + C_{11} \phi_1' + C_{12} \phi_1 + C_{13} \phi_2'' + C_{14} \phi_2 = 0 \quad (13)$$

$$C_{15} u' + C_{16} v + C_{17} \phi_1'' + C_{18} \phi_1 + C_{19} \phi_2'' + C_{20} \phi_2' + C_{21} \phi_2 = 0 \quad (14)$$

where the angular velocities ω_1 and ω_3 have been nondimensionalized as follows:

$$u = LM \omega_3 / \bar{M} r_1 \Omega; \quad v = LM \omega_1 / \bar{M} r_1 \Omega$$

and the constant coefficients can be related to the parameters according to

$$\begin{aligned}
C_1 &= 1.0; \quad C_2 = [\bar{B} - \bar{A} + I_{R2} s / \Omega] / \bar{A} \\
C_3 &= -m(LM/\bar{M})^2 / \bar{A} \\
C_4 &= -C_3; \quad C_5 = -C_2; \quad C_6 = 1.0; \quad C_7 = 2C_3 \\
C_8 &= -1.0; \quad C_9 = 1.0 \\
C_{10} &= 1 - m[1/\bar{M} + (r_0 + r_1)^2/B]; \quad C_{11} = \bar{k} \\
C_{12} &= r_0/r + m/\bar{M} + \bar{K}; \quad C_{13} = 2m/\bar{M} - 1 + C_{10} \\
C_{14} &= -m/\bar{M}; \quad C_{15} = 1.0; \quad C_{16} = -1.0; \quad C_{17} = C_{13} \\
C_{18} &= C_{14}; \quad C_{19} = C_{10}; \quad C_{20} = C_{11}; \quad C_{21} = C_{12}
\end{aligned}$$

The prime indicates differentiation with respect to the dimensionless time τ where $\tau = \Omega t$. Equations (11-13) are valid for $N = 1$ damper, while Eqs. (11-14) describe the system when $N = 2$.

B. Stability Criteria

The stability criteria of Routh-Hurwitz⁵ yield the necessary and sufficient conditions for the stability of this linear system. Likins and Mingori⁶ have recently discussed the difficulties in applying Lyapunov techniques to freely spinning systems, pointing out that this method will yield both necessary and sufficient conditions for stability only when the system damping is complete in all the indicated state variables. Since the Routh-Hurwitz algorithms will always yield both necessary and sufficient stability criteria for a constant coefficient system regardless of the coordinates selected, it was decided to use this more traditional approach.

For stability of the small amplitude oscillations it is found that positive damping must be present and in addition if $C_2 > 0$, the only other condition not automatically nor trivially satisfied is

$$C_2 \left[C_2 \left(\frac{r_0}{r} + \frac{2m}{\bar{M}} + \bar{K} \right) - 2m \frac{(L/M/\bar{M})^2}{\bar{A}} \right] > 0 \quad (15)$$

If $C_2 > 0$, i.e.,

$$\bar{B} + I_{R2} s / \Omega - \bar{A} > 0 \quad (16)$$

the term in brackets in Eq. (15) must be positive or,

$$r_0/r_1 + 2m/\bar{M} + \bar{K} > 2m(LM/\bar{M})^2/(\bar{B} - \bar{A} + I_{R2} s / \Omega) \quad (17)$$

It is interesting to note that Eq. (16) will be satisfied if 1) the nominal spin axis of the main satellite is the axis of maximum inertia and the rotor is a) spinning in the positive sense, b) not spinning at all, or c) spinning very slowly in the negative sense (positive sense implies a rotor spin with the main body spin); or 2) the nominal spin axis of the main satellite is the axis of minimum moment of inertia and the rotor is spinning rapidly in the positive sense, compared with the nominal main body angular velocity Ω . If only one pendulum is uncaged, then inequality Eq. (17) becomes

$$r_0/r_1 + m/\bar{M} + \bar{K} > m(LM/\bar{M})^2/(\bar{B} - \bar{A} + I_{R2} s / \Omega) \quad (18)$$

In this case, a second stationary mass m might be placed on

the rim opposite the null position of the free damper to provide a dynamic balance when ϕ_1 is small. This counter mass could, for example, be the end mass associated with a second (caged) pendulum. The stability criteria presented here correspond identically to those given by Haseltine¹ when the effects of the torsion wire and of the rotor are omitted.

For the case when $C_2 < 0$, it is seen that condition Eq. (15) is automatically satisfied. The principal necessary and sufficient conditions for stability in addition to positive damping are

$$C_2 < -1 \tag{19}$$

$$\frac{r_0}{r_1} + \frac{m}{\bar{M}} + \bar{K} + C_2^2 \frac{m}{\bar{A}} \left(\frac{LM}{\bar{M}}\right)^2 > \frac{3m}{\bar{A}} \left(\frac{LM}{\bar{M}}\right)^2 |1 + C_2| \tag{20}$$

while the following necessary condition must also be satisfied:

$$r_0/r_1 + m/\bar{M} + \bar{K} + C_2^2 C_{10} > (3m/\bar{A})(LM/\bar{M})^2 |1 + C_2| \tag{21}$$

When the system has two dampers free to move, m should be replaced by $2m$ in conditions (20) and (21). Typically $m/\bar{M} \ll 1$ and $C_{10} \approx 1.0$; thus condition (20) is the stronger condition for $C_2 \ll -1$. The significance of condition (19) is that if the main part of the satellite is spinning about the axis of maximum inertia, and if the rotor spin is opposite in sense to that of the main body, stability is insured only for high rotor spin rates.

The system characteristic equation was developed for the case of one damper (with counterweight) and for the case of two freely moving dampers. For the case of the single damper, a fourth-order polynomial results in terms of the original constants

$$f(s) = (C_{10} + C_3)s^4 + C_{11}s^3 + [C_{12} + C_2^2 C_{10} - 3C_3(1 + C_2)]s^2 + C_2^2 C_{11}s + C_2(C_2 C_{12} + C_3) = 0 \tag{22}$$

For the case of two dampers, the characteristic equation is a sixth order polynomial having a pair of separable damped normal modes of oscillation with the frequency λ where

$$\lambda = \frac{(r_0/r_1 + \bar{K})^{1/2} \Omega}{\{[1 - 2m(r_0 + r_1)/\bar{B}]\}^{1/2}}$$

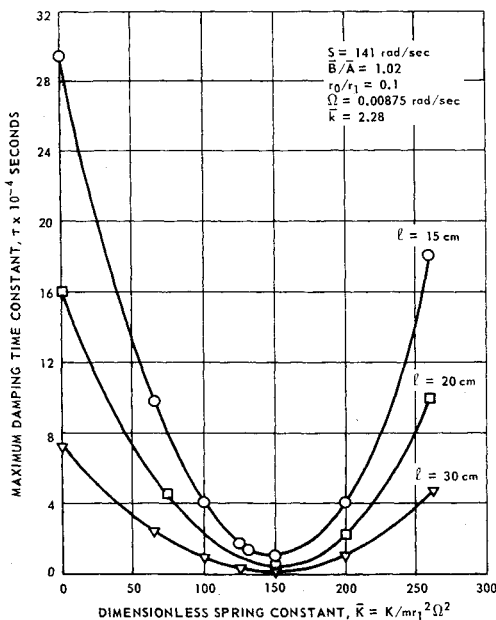


Fig. 3 Variation of maximum damping time constant with spring constant (rotor on).

It appears, therefore, that the inherent undesirable effects associated with forced resonance could be avoided by reverting to the single pendulum case. If not, care should be taken in the design such that $\lambda/\Omega \neq (N)^{\pm 1}$; and also: $\lambda \neq (N)^{\pm 1} \omega_0$, where N is an integer, to preclude forced motion by perturbations induced at harmonics of the orbital frequency. It should be noted that redundancy could still be achieved by using a second collinearly mounted pendulum as a counterweight, with the provision that either damper may be caged so that only one is free to move at a given time.

III. Numerical Results

A. Optimization of Damping System Parameters

The roots of the characteristic polynomial Eq. (22) were determined with a computer routine using parameters considered representative during the early design phase of SAS-A. The satellite was considered to have a mass of 114 kg, a polar moment of inertia of 20.4 kg-m², and a transverse moment of inertia of 20.0 kg-m². The rotor moments of inertia were taken to be 0.015 kg-m² (polar) and 0.00775 kg-m² (transverse); the mass of the rotor is assumed to be incorporated within the 114 kg. These moments of inertia give a composite ratio of polar moment of inertia to transverse moment of inertia of 1.02 (denoted by \bar{B}/\bar{A}). The length of the pendulum was fixed at 20 cm while the distance from the pivot point to the polar axis was considered to be 2 cm, thus giving a ratio r_0/r_1 of 0.1. The pendulum end mass was selected as 0.25 kg. The remaining physical parameters were varied in a systematic manner to give the best damping (i.e., maximum damping of the least damped normal mode of oscillation).

Figure 3 shows the variation of the damping time constant corresponding to the least damped mode with variations in the torsion wire spring constant and with variations in the height of the plane of the damper. The constant speed rotor was assumed to be operating at a relative spin rate of 141 rad/sec with the nominal spin rate of the main satellite of 0.00875 rad/sec. The improvement in damping performance with increased height of the damper plane l is noted. However, as l is increased, care must be exercised to see that the stability criteria Eq. (18) is not violated; an upper limit on this height with the present set of parameters appears to be about 50 cm. In addition, restrictions on the payload dimensions would also limit this parameter. From the figure it appears that the optimum dimensionless spring constant is between 125 and 150 with the best damping time constants of the least damped mode of about 40 min for $l = 30$ cm.

The next study was conducted to determine the optimum damping rate constant using a value of $\bar{K} = 130.6$ (or $K = 1 \times 10^{-4}$ nt-m/rad with the aforementioned parameters). The results of this study are given in Fig. 4 for three different

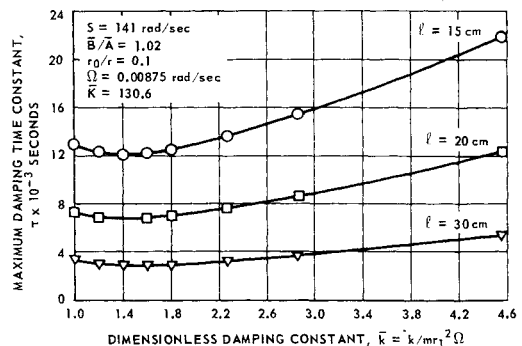


Fig. 4 Variation of maximum damping time constant with damping rate constant (rotor on).

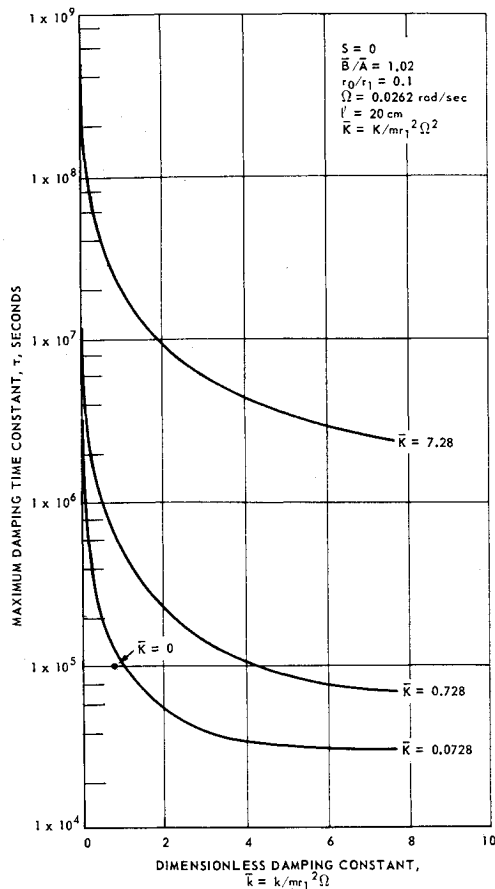


Fig. 5 Variation of maximum damping time constant with spring constant and damping rate constant (rotor off).

damper plane heights. The rotor and main body spin rates are the same as in Fig. 3. It is seen that the maximum time constant has a less pronounced minimum than in the previous case with values of \bar{k} between 1.0 and 2.2 appearing to give optimum performance. A value of $\bar{k} = 1.0$ corresponds to a dimensional damping rate constant of 0.875×10^{-4} nt-m-sec/rad for the present set of parameters.

In the event of failure of the rotor system it is important to maintain the stability of the system and at the same time optimize the damping system performance. It is noted that to maintain stability in the event of rotor failure either $C_2 > 0$ or $C_2 < -1.0$. From design consideration of the SAS-A satellite where there is little difference between the polar and transverse moments of inertia, it is clear that $C_2 > 0$ is the criteria to be considered. Thus from Eq. (16), $\bar{B}/\bar{A} > 1.0$ which means that the nominal spin axis of the main satellite must now be the axis of greatest inertia.

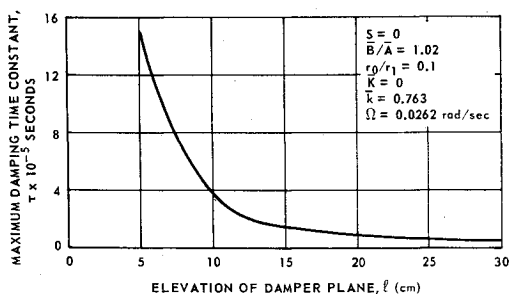


Fig. 6 Variation of maximum damping time constant with elevation of damper plane (rotor off).

Figure 5 illustrates the variation of the maximum damping time constant with changes in both the spring constant and damping rate constant under the assumption that the rotor has been turned off. The degradation in damping performance is immediately apparent as the best time constants are at least an order of magnitude greater than those shown in Figs. 3 and 4. It is seen that the best damping performance is obtained with the spring constant as small as possible. Furthermore, the damping is not significantly improved by increasing the dimensionless damping rate constant beyond 3.0. It should be noted that with the rotor off the nominal main body spin rate will be increased by a factor of three to further improve damping performance. The capability to vary the spring constant (or stiffness of the torsion wire) is strongly recommended in order to improve the damping characteristics in the event of rotor failure.

Figure 6 verifies that with the rotor off the improvement in damping with increased height of the plane of the damper is also maintained. When $l = 0$, it can be seen from examination of Eqs. (6-9) that the first-order coupling between the motion of the dampers and the transverse angular velocities of the main satellite is removed.

The results from these parametric studies of the linearized equations of motion were used as a basis for input parameters to the Dynamic Simulation Computer Program. This program numerically integrates the nonlinear equations of motion of a dual-spin satellite with a pendulous nutation damper system. The main limiting assumption in this model is the small amplitude motion of the nutation damper; the program has been modified to include the presence of mechanical stops which limit the damper displacement amplitude to $\pm 20^\circ$.

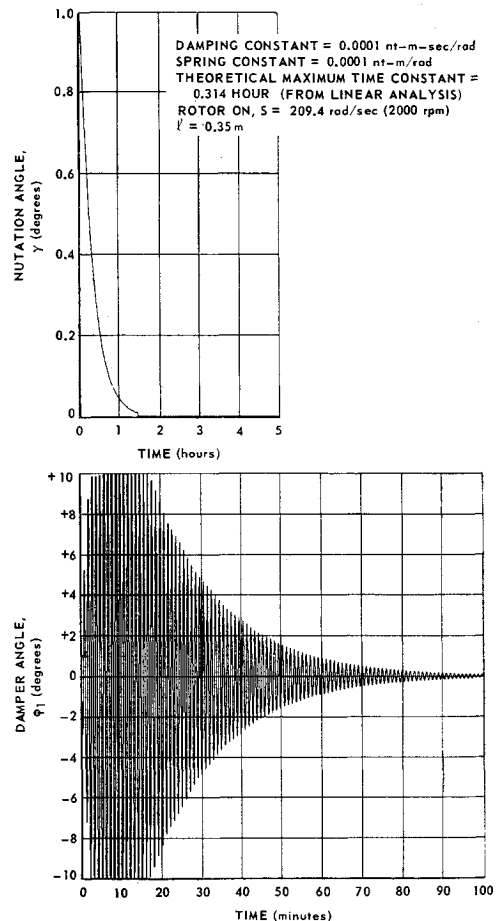


Fig. 7 Transient response for initial nutation angle of one degree (rotor on).

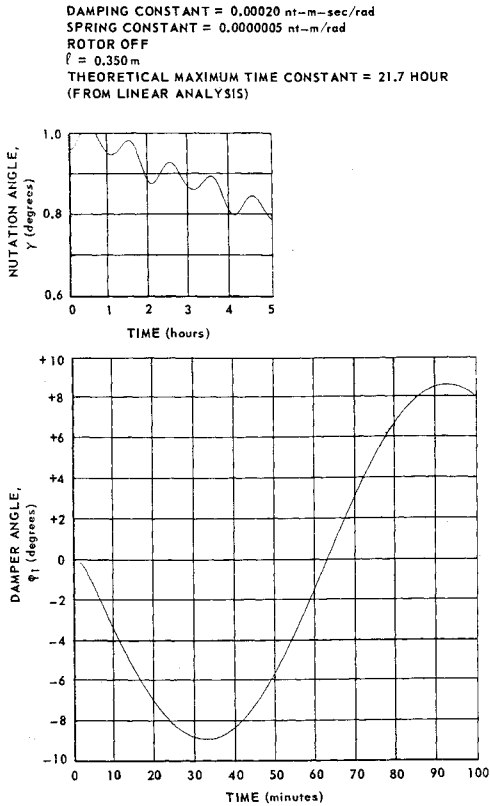


Fig. 8 Transient response for initial nutation angle of one degree (rotor off).

This study of the transient response of the attitude was made to observe the behavior of the damper angle and the decay of the nutation angle (angle between the spin axis of the body and the total angular momentum vector of the system). Several runs were simulated varying the spring constant, damping constant, and setting the rotor on or off. External perturbations such as magnetic and gravity-gradient torques on the main body were set to zero.

Figures 7 and 8 show the transient response for an initial nutation angle of 1 degree. Figure 7 represents the optimum nutation decay with the rotor on, whereas Fig. 8 illustrates a case near optimum with the rotor off. The following quantities were used as common input and represented early SAS-A design parameters: $M = 114$ kg; $I_{b_2} = 20.8$ kg-m²; $I_{b_1} = I_{b_3} = 20.00$ kg-m²; $I_{R_2} = 0.0101$ kg-m²; $I_{R_1} = I_{R_3} = 0.00508$ kg-m²; $m = 0.2126$ kg; $r_1 = 0.203$ m; $r_0 = 0.025$ m.

The varied parameters for each case are indicated in each figure, respectively. The difference in the time scale between the transient response of the damper motion and the transient response of the nutation angle should be noted in Figs. 7 and 8. The transient response of all major parameters was observed over a five-hour period from initialization of the problem. Because the observation of the nutation angle decay was the principal objective of this study, it was decided to adjust the CALCOMP computer routine accordingly to plot only the nutation response over the full five hour period.

It can be seen that the time constants obtained from the decay of the nutation angle are in no cases larger than the values predicted for the least damped mode of the linearized system. (The time constant associated with nutation angle decay is the time required for the nutation angle amplitude to decrease to $1/e$ of its initial value).

B. Pointing Error Study for SAS-A with Asymmetry

The numerical results presented to this point have been based on the assumption that the main body axes of sym-

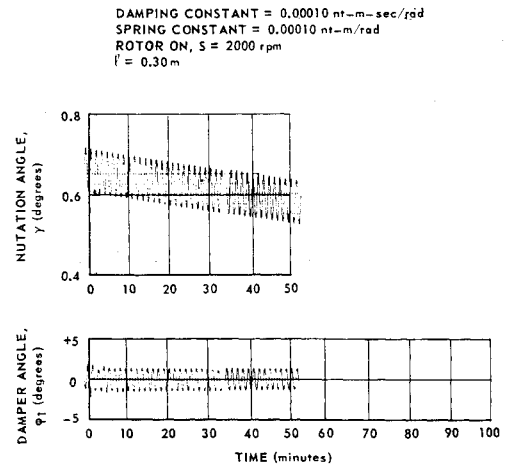


Fig. 9 Transient response for the case of initial transverse body angular rates.

metry are also principal axes of inertia. Results of mass balance tests have shown that there is a small unsymmetrical distribution of the satellite's mass with respect to this coordinate system. A preliminary spin axis pointing error study was made to determine the effects of dynamic mass unbalance of the satellite main body in a torque-free environment (without gravitational torques), and to see whether these effects are within the mission specifications.⁷ This was accomplished with the attitude dynamics computer simulation which numerically integrates the nonlinear equations of motion.

A representative set of moments and products of inertia were used in the simulation. After a suitable similarity transformation the elements of the moment of inertia tensor expressed in the main body symmetry axis system ($\bar{b}_1, \bar{b}_2, \bar{b}_3$) were calculated to be in units of kg-m²: $I_{11} = 28.07$; $I_{12} = 0.220$; $I_{13} = 0.070$; $I_{21} = I_{12}$; $I_{22} = 31.13$; $I_{23} = -0.095$; $I_{31} = I_{13}$; $I_{32} = I_{23}$; $I_{33} = 27.43$, where \bar{b}_2 is the nominal spin axis.

The problem was initialized for several cases. The satellite mass, pendulum end mass, the rotor inertia characteristics, the lengths of the pendulum arm, and the displacement of the damper pivot point from the \bar{b}_2 axis were the same as listed for Figs. 7 and 8. Other parameters that were common to all cases considered here were: $l = 0.30$ m; $\epsilon = 2000$ rpm (209 rad/sec); $\Omega = \frac{1}{2}$ rpm; $k = 1 \times 10^{-4}$ nt-m-sec/rad; $K = 1 \times 10^{-4}$ nt-m/rad.

For this pointing error study, one is interested in the following parameters whose definitions are given⁷:

- 1) The coning or nutation angle γ (gamma). (The angle between the total angular momentum vector of the system and the spin axis \bar{b}_2).
- 2) $\Delta\theta_i$ = an angle between any two spin axis pointing vectors taken at different time intervals. $\Delta\theta_i$ is comprised of contributions due to the following two effects—a) the nominal change in direction of $\bar{\omega}_2$ with respect to the invariant line (\bar{L}) as the body cone rolls about the space cone in

Table 1 Comparison of simulated and computed steady-state coning angle

Case	Cross product of inertia programed, kg-m ²	Steady-state coning angle	
		Simulated	Computed
1	$I_{12} = I_{21} = 0.22$	0.05°	0.047°
2	$I_{22} = I_{23} = 0.0948$	0.02°	0.02°
3	$I_{31} = I_{13} = 0.0701$	0°	0°
4	All of the above	0.055°	0.055°

Table 2 Study results

	Allowed	Simulated
γ	0.2°	0.055° ± 0.025°
$\Delta\theta_i$	1.5 arc min/20 sec time	1.0 arc min/20 sec time

accordance with the Poinot construction concept⁸ for a symmetrical satellite, and b) the deviation (wobble) in the motion of $\bar{\omega}_2$ from a) due to mass asymmetry where the \bar{b}_2 axis is no longer a principal axis of inertia.

As a check on the simulation, the computer program was initialized for several cases that could be easily verified by hand computation. The spacecraft was given zero initial transverse angular body rates and each of the cross products of inertia was programmed in turn to observe their effect on the coning angle. The coning angle can be approximated for zero transverse angular body rates and a torque-free environment by $\tan\gamma \approx [(L_1^2 + L_3^2)/L_2^2]^{1/2}$ where $L_1 = -I_{12}\omega_2$; $L_2 = I_{22}\omega_2 + I_{R2S}$; $L_3 = -I_{32}\omega_2$. The results are summarized in Table 1.

Case 4 is indicative of the nominal steady state motion of the system in a torque-free environment. The small sinusoidal variation about the steady-state cone angle of $\pm 0.025^\circ$ that was observed can be attributed to a cyclic gyroscopic precession torque. This torque results when a component of the rotor reaction torque on the main satellite is at right angles to the satellite's angular momentum vector.

To observe the transient behavior, the satellite was given an initial transverse angular body rate to simulate a nominal cone angle of 0.65° . Figure 9 shows that the initial rate of decay of the coning angle (γ) is on the order of 0.1° per hour. Comparison with the transient decay of γ shown in Fig. 7 for the case of mass symmetry, indicates that the simulated mass asymmetry degraded the performance of the nutation damper by a factor of almost ten.

The sensitivity of the nutation damping system performance to changes in the moments of inertia was also supported by results of a parametric study of the linearized equations of motion with mass symmetry for a different configuration. In this study the moment of inertia ratio (ratio of polar moment of inertia to the transverse moment of inertia) was varied as were the spring constant and damping constant of the system. These results, indicate that an increase of 6% in the moment of inertia ratio can decrease the damping time constant by at least a factor of three.³

The $\Delta\theta_i$ predictability was computed for the worst case, assuming that the sense of rotation about the nominal spin axis was opposite to that of the steady-state precession, that the coning angle was a maximum of 0.075° , and that the period of spin axis precessional motion was 6 min.

The results of the study to examine the effects of mass asymmetry on the orientation of the nominal spin axis are summarized in Table 2.

For the values of mass asymmetry given and for a torque-free environment, the satellite is predicted to perform within the specified limits of γ and $\Delta\theta_i$. However, the addition of gravity-gradient, aerodynamic, and solar pressure torques to the simulation will provide more realistic evaluation of γ , $\Delta\theta_i$, and the spin axis drift rate. In addition, the presence of mass asymmetry noticeably degrades the performance of the nutation damping system.

IV. Conclusions

As a result of the present analysis and numerical results the following conclusions can be made in conjunction with the design of the dual-spin attitude control system considered here:

1) System performance is optimized by using only one of the two pendulous dampers at a time. If redundancy is desired, the second (caged) damper could serve as a balance. In addition the capability of varying the stiffness of the torsion wire support will result in greatly improved damping in the event of rotor failure.

2) For the case there is little difference between the polar and transverse moments of inertia of the main satellite, system instabilities may result when the rotor is spinning very slowly in the negative sense, i.e., the rotor angular momentum vector is opposite in sense to the direction of main body angular momentum.

3) The predicted minimum time constants of the least damped normal mode of oscillation with the rotor on and no mass asymmetry are under 40 min; the predicted minimum time constants when the rotor is off and the spring constant adjusted are between 20 and 30 hr.

4) The simulated effects of mass unbalance of the satellite in a torque-free environment indicate that the steady state amplitude of the coning or nutation angle of $0.055 \pm 0.025^\circ$ is within the allowable amplitude of 0.2° . In addition, the maximum angle between any two spin axis pointing vectors taken at 20 sec time intervals is slightly less than the allowable 1.5 min of arc. The presence of mass asymmetry degrades the optimum performance of the nutation damping system (i.e., maximum time constant), by approximately an order of magnitude, with the set of moments and products of inertia used in this study.

References

- Haseltine, W. R., "Nutation Damping Rates for a Spinning Satellite," *Aerospace Engineering*, Vol. 21, No. 3, March 1962, pp. 10-17.
- Proceedings of the Symposium on Attitude Stabilization and Control of Dual Spin Spacecraft*, Rept. TR-0158 (3307-01)-16, Nov. 1967, Aerospace Corp.
- Bainum, P. M., Fuechsel, P. G., and Mackison, D. L., "On the Motion and Stability of a Dual-Spin Satellite with Nutation Damping," TG-1072, June 1969, Applied Physics Lab., Johns Hopkins Univ., Silver Spring, Md.
- Whittaker, E. T., *A Treatise on the Analytical Dynamics of Particles and Rigid Bodies*, 4th ed., Cambridge University Press, Cambridge, England, 1959, pp. 41-44.
- McCuskey, S. W., *An Introduction to Advanced Dynamics*, Addison-Wesley, Reading, Mass., 1959, pp. 182-187.
- Likins, P. W. and Mingori, D. L., "Lyapunov Stability Analysis of Freely Spinning Systems," XVIII Congress-International Astronautical Federation, Belgrade, Yugoslavia, September 1967; also *Congress Proceedings*, to be published.
- Zitterkopf, D. L., "SAS-A System Design and Interface Document," S2-0-43A, April 30, 1968, Applied Physics Lab., Johns Hopkins Univ., Silver Spring, Md.
- McCuskey, S. W., *An Introduction to Advanced Dynamics*, Addison-Wesley, Reading, Mass., 1959, pp. 129-134.